Supporting Information

Janus graphene oxide sponges for high-purity fast separation of both water-in-oil and oil-in-water emulsions

Jongju Yun, [†,+,⊥] *Fakhre Alam Khan,* [‡,⊥] *and Seunghyun Baik*[‡,§,*]

[†] Department of Energy Science, Sungkyunkwan University, Suwon, 16419, Republic of Korea

[‡] School of Mechanical Engineering, Sungkyunkwan University, Suwon, 16419, Republic of Korea

[§] Center for Integrated Nanostructure Physics, Institute for Basic Science (IBS), Suwon 16419, Republic of Korea

[+] Present address: Technical Research Ceter, Daelim Heat Co., LTD, Gimpo, 10045, Republic of Korea

***e-mail: sbaik@me.skku.ac.kr**

[⊥]These authors contributed equally to this research work.

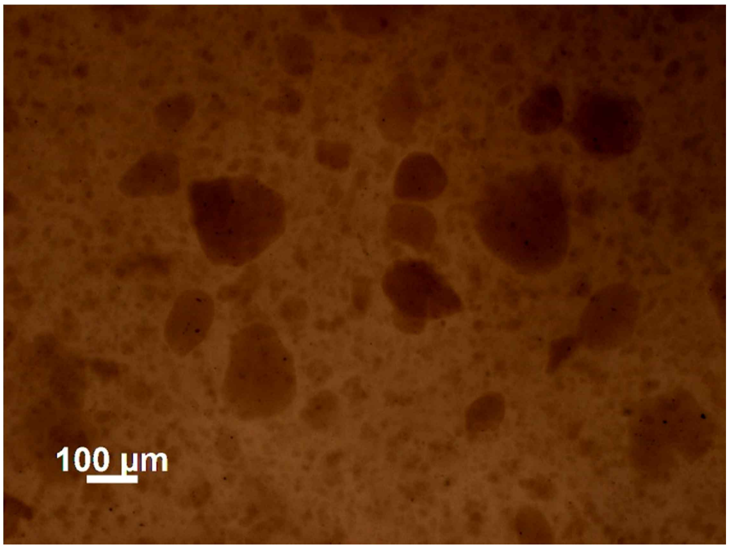

Figure S1. An optical microscopic image of GO flakes dispersed in deionized water after bath sonication (200 W, 3 h). The average size of dispersed GO flakes was 70~110 μm.

Optimization of the synthesis process of R-GO sponge

A number of different synthesis conditions were explored to optimize the R-GO sponge. Two different reducing agents (sodium bisulfite and ascorbic acid) were tested.[1-2] The heating temperature (80, 95, 110, or 130°C), heating duration (2, 3, 4, 5, or 6 h), and mixing ratio between GO dispersion and aqueous reducing agent (1:1, 1:2, 1:3, 1:4, 1:5, or 1:6) were also varied. The optimized condition was described in detail in the Experimental section (ascorbic acid, heating temperature = 110°C, heating time = 3 h, mixing ratio = 1:5). Figure S2 shows R-GO sponges synthesized at different heating temperatures and durations. The reducing agent was ascorbic acid.

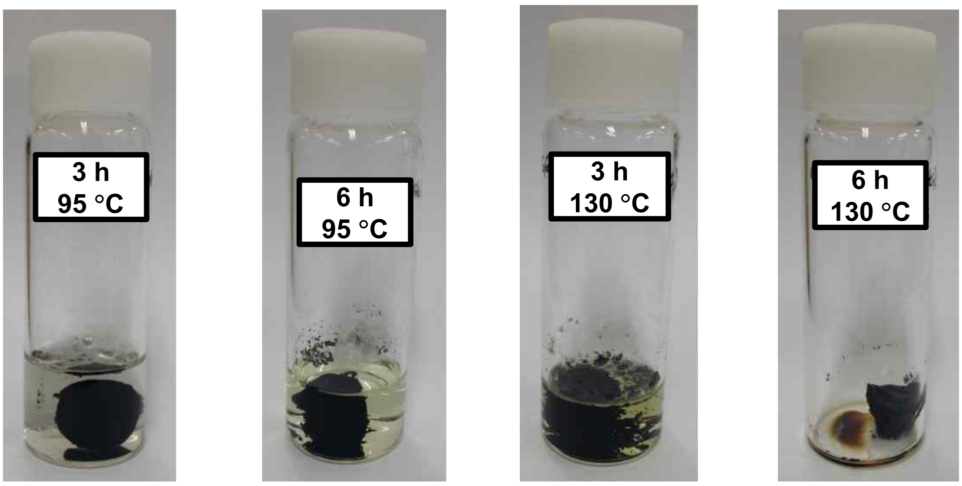

Figure S2. R-GO sponges synthesized at different heating temperatures and durations. The mixing ratio between GO dispersion and ascorbic acid was 1:5.

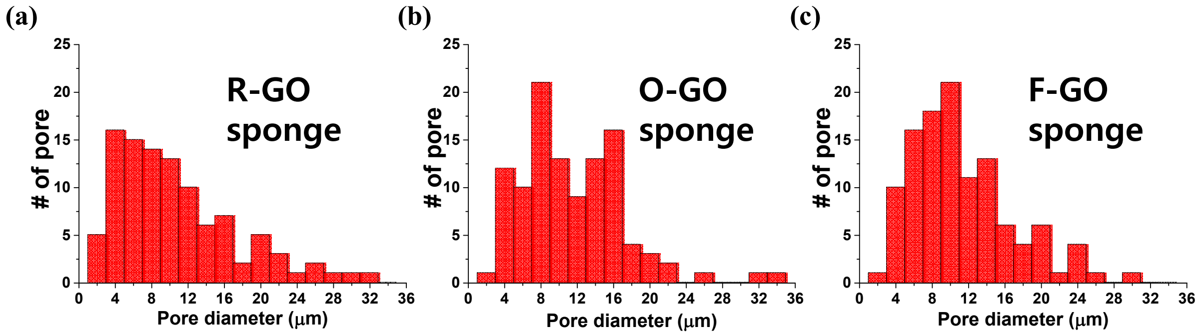

Figure S3. The pore size distribution of R-GO (a), O-GO (b), and F-GO (c) sponges.

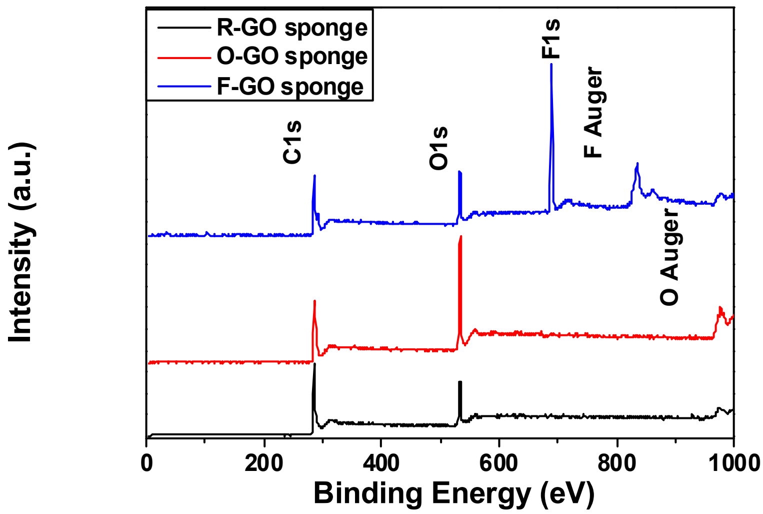

Figure S4. XPS spectra of R-GO, O-GO, and F-GO sponges.

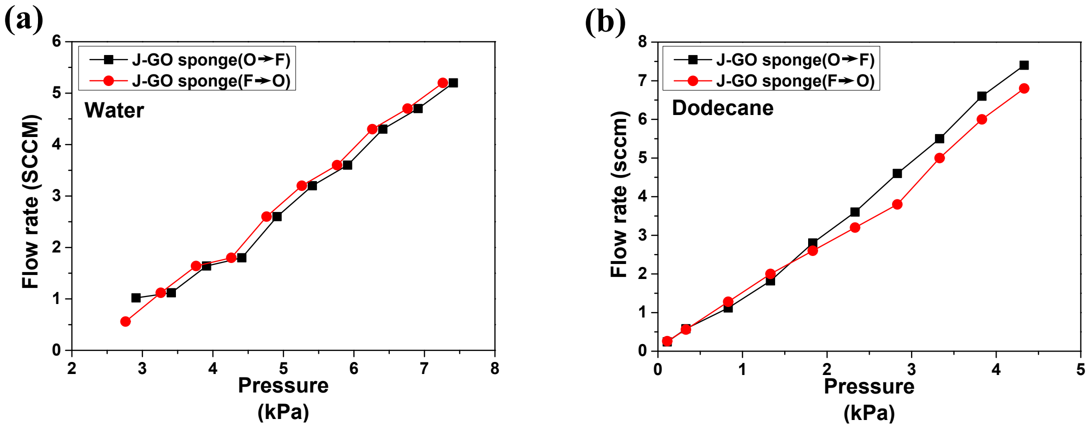

Figure S5. Comparison of the experimental flow rates through the J-GO sponge depending on the flow direction. (a) Water. (b) Dodecane.

Oil type	Structure	Molecular weight (g mol^{-1})	Viscosity at 25 °C(Pa·s)
Xylene	$C_6H_4(CH_3)_2$	106.17	6.20 x 10^{-4}
Cyclohexane	C_6H_{12}	84.16	9.80 x 10^{-4}
Dodecane	$CH_3(CH_2)_{10}CH_3$	170.33	1.34 x 10^{-3}
Hexadecane	$CH_3(CH_2)_{14}CH_3$	226.44	3.04 x 10^{-3}

Table S1. Physical properties of oils.

No	Membrane type	Material	Pore size	Permeability ($m^3 \cdot m \cdot m^{-2} \cdot s^{-1} \cdot Pa^{-1}$)	Reference
1	Nanotubes	Multiwalled carbon nanotubes	7 nm	1.49×10^{-13}	3
2			7 nm	1.60×10^{-13}	4
3		Doublewalled carbon nanotubbes	1.3-2 nm	1.58×10^{-15}	5
4	Porous membrane	GO	1 nm	3.60×10^{-16}	6
5		Nanostrand-channeled GO	3-5 nm	3.87×10^{-14}	
6		Poly(ethylene glycol)-coated fritted glass fiber	10-20 µm	3.56×10^{-16}	7
7			70-100 µm	2.25×10^{-15}	
8			145-174 µm	5.08×10^{-15}	
9		Graphene	50 nm	9.52×10^{-18}	8
10	Metal Foam	Nickle-Chromium	400 µm	1.57×10^{-6}	9
11		Nickel	360 µm	3.94×10^{-7}	
12		Aluminum	75 µm	1.38×10^{-9}	10
13		Aluminum	400 µm	4.54×10^{-7}	
14		Nickel	500 µm	1.83×10^{-6}	11
15		Copper	1000 µm	6.97×10^{-6}	
16	R-GO sponge	GO	11µm	9.19×10^{-11}	This work
17	O-GO sponge		11µm	2.41×10^{-9}	
18	F-GO sponge		11µm	2.99×10^{-10}	
19	J-GO sponge		11µm	1.20×10^{-9}	

Table S2. The permeabilities of water through GO sponges (this study) were compared with the data in literatures.

Fluid permeation through the R-GO sponge (pore size: 94.1 μm)

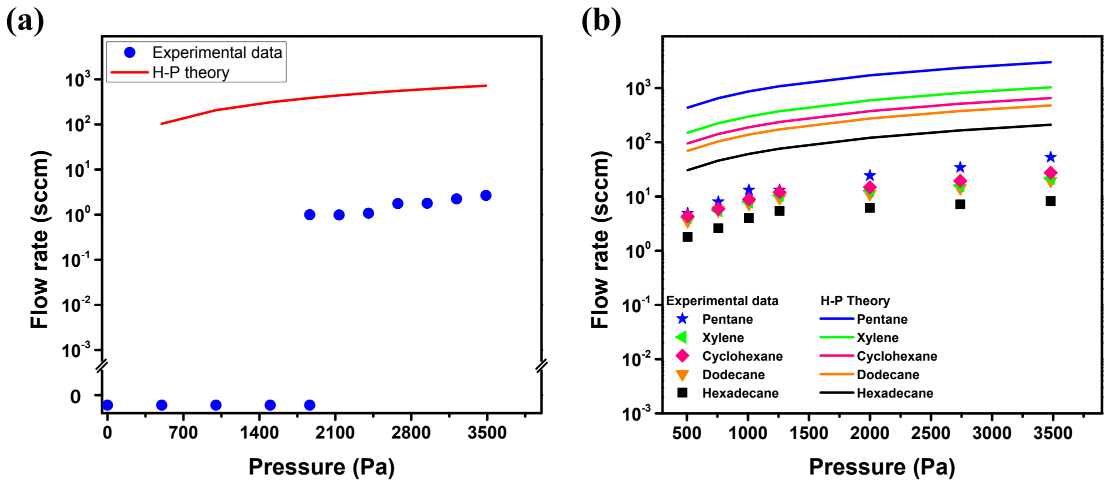

Figure S6. Comparison of the experimental flow rates and Hagen-Poiseuille theory for water (a) and oils (b) as a function of the pressure difference across the R-GO sponge membrane (pore size: 94.1 μm).

Figure S6a compares experimentally-measured water flow rates through the R-GO sponge with the Hagen-Poiseuille theory. The Hagen-Poiseuille prediction was calculated under the assumption of straight circular pipe (Equation (6)). The theory over-predicted the experimental flow rate. This could be due to the random, non-straight flow passage through the R-GO sponge. Interestingly, the experimentally-observed water flow was initiated when a pressure greater than 1864 Pa was applied (i.e. intrusion pressure), which was not consistent with the Hagen-Poiseuille theory. The oil flow rates calculated from the Hagen-Poiseuille theory were also greater than the experimentally-measured flow rates (Figure S6b). The oils were immediately absorbed and passed through the R-GO sponge when the amount greater than the sorption capacity was supplied. This was due to the excellent wettability of oil on the R-GO sponge, and the capillary pressure of the liquid meniscus inside the pores worked on the forward direction.

Water permeation repeatability through the R-GO sponge (pore size: 94.1 μm)

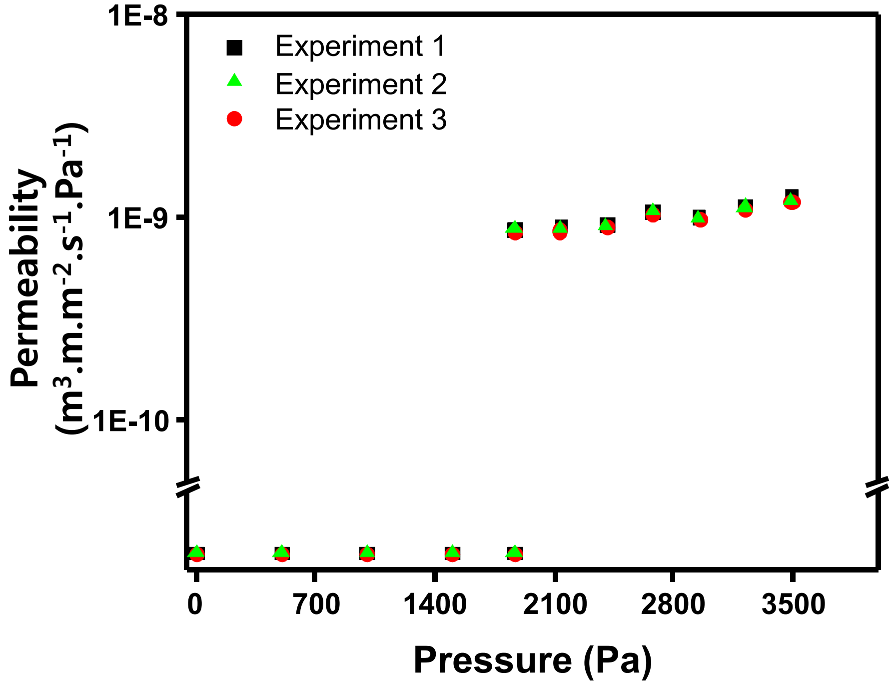

Figure S7. Water permeation repeatability through the R-GO sponge.

The water permeation experiment was carried out 3 times using the same R-GO sponge. The R-GO sponge could be re-used again after drying in air, and the repeatability was excellent.

Water-in-oil emulsion separation using R-GO sponge (pore size: 94.1 μm)

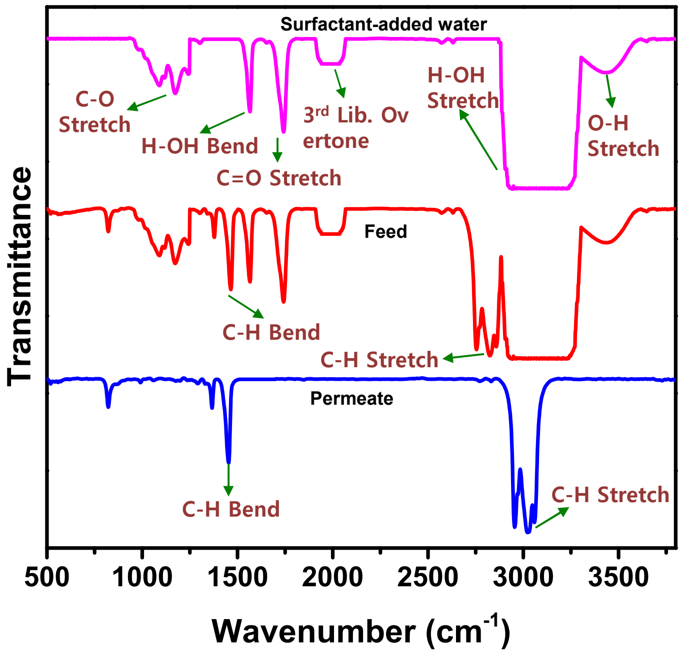

Figure S8. FT-IR spectra of the surfactant-added water, surfactant-stabilized water-in-oil emulsion (feed), and separated permeate using the R-GO sponge (pore size: 94.1 μm).

The surfactant-stabilized water-in-oil emulsion was prepared (deionized water: dodecane: Span-80 = 10: 89.5: 0.5 vol%). After the first separation process at the applied pressure drop of 700 Pa, the color of permeate was somewhat opaque indicating incomplete separation. The flow was stopped when enough permeate was obtained for the second iteration experiment. A clear transparent permeate could be obtained after the second separation process, at the applied pressure drop of 640 Pa, indicating no presence of water. The purity of separated oil measured by the titration method was 99.4 %. The purity of separation was also investigated by FTIR analysis (Figure S8). The characteristic peaks of Span-80 (C-O, C=O, and O-H stretching bands at 1090, 1168, 1740, and 3400 cm^{-1}) as well as characteristic water peaks were observed in the surfactant-added deionized water.[12] The surfactant-stabilized water-dodecane feed emulsion retained all the characteristic peaks of constituents. The peaks of permeate after the second repeated separation were identical to those of the pure dodecane demonstrating excellent oil separation performance of the R-GO sponge. It is interesting to note that only dodecane passed through the R-GO sponge, and surfactant remained in the water-in-oil mixture on the feed side during the separation experiments. The hydrophilic-lipophilic balance (HLB) of Span-80 was 4.3, and both oil and water were required to maintain high solubility. The high purity separation of water-in-oil emulsion was achieved by the R-GO sponge at a low pressure drop (640~700 Pa) which is advantageous for the energy-efficient water-oil separation in industry.

REFERENCES

1. Zhang, X.; Sui, Z.; Xu, B.; Yue, S.; Luo, Y.; Zhan, W.; Liu, B. Mechanically Strong and Highly Conductive Graphene Aerogel and its Use as Electrodes for Electrochemical Power Sources. *J. Mater. Chem.* **2011,** *21*, 6494-6497.

2. Chen, W.; Yan, L. In Situ Self-assembly of Mild Chemical Reduction Graphene for Three-dimensional Architectures. *Nanoscale* **2011,** *3*, 3132-3137.

3. Majumder, M.; Chopra, N.; Andrews, R.; Hinds, B. J. Nanoscale Hydrodynamics: Enhanced Flow in Carbon Nanotubes. *Nature* **2005,** *438*, 44-44.

4. Majumder, M.; Chopra, N.; Hinds, B. J. Mass Transport Through Carbon Nanotube Membranes in Three Different Regimes: Ionic Diffusion and Gas and Liquid Flow. *ACS Nano* **2011,** *5*, 3867-3877.

5. Holt, J. K.; Park, H. G.; Wang, Y.; Stadermann, M.; Artyukhin, A. B.; Grigoropoulos, C. P.; Noy, A.; Bakajin, O. Fast Mass Transport Through Sub-2-Nanometer Carbon Nanotubes. *Science* **2006,** *312*, 1034-1037.

6. Huang, H. B.; Song, Z. G.; Wei, N.; Shi, L.; Mao, Y. Y.; Ying, Y. L.; Sun, L. W.; Xu, Z. P.; Peng, X. S. Ultrafast Viscous Water Flow Through Nanostrand-Channelled Graphene Oxide Membranes. *Nat. Commun.* **2013,** *4,* 2979.

7. Howarter, J. A.; Youngblood, J. P. Amphiphile Grafted Membranes for the Separation of Oil-in-Water Dispersions. *J. Colloid Interface Sci.* **2009,** *329*, 127-132.

8. Celebi, K.; Buchheim, J.; Wyss, R. M.; Droudian, A.; Gasser, P.; Shorubalko, I.; Kye, J. I.; Lee, C.; Park, H. G. Ultimate Permeation Across Atomically Thin Porous Graphene. *Science* **2014,** *344*, 289-292.

9. Khayargoli, P.; Loya, V.; Lefebvre, L.; Medraj, M. In *The Impact of Microstructure on the Permeability of Metal Foams*, CSME forum, **2004**; pp 220-228.

10. Despois, J.-F.; Mortensen, A. Permeability of Open-Pore Microcellular Materials. *Acta Mater.* **2005,** *53*, 1381-1388.

11. Bonnet, J.-P.; Topin, F.; Tadrist, L. Flow Laws in Metal Foams: Compressibility and Pore Size Effects. *Transp. Porous Media* **2008,** *73*, 233-254.

12. Fu, X.; Kong, W.; Zhang, Y.; Jiang, L.; Wang, J.; Lei, J. Novel Solid–Solid Phase Change Materials with Biodegradable Trihydroxy Surfactants for Thermal Energy Storage. *RSC Adv.* **2015,** *5*, 68881-68889.